

## The Color-Magnitude Diagram of composite stellar populations

Laura Greggio

*Osservatorio Astronomico, Via Ranzani 1, 40127 Bologna, Italy*

### Abstract.

The theoretical relation between the number of post main sequence stars from stellar populations and their total mass is investigated. This is used to derive some basic relations between the stellar number counts of stellar populations with an age spread and the star formation history which produced them. The main purpose of this investigation is to offer a guideline for the construction of simulations aimed at reproducing color-magnitude diagrams.

### 1. Introduction

Theoretical simulations of Color-Magnitude Diagrams (CMD) have proven very successful to investigate the Star Formation History (SFH) of nearby galaxies (see the contributions by Aparicio and by Tosi et al. in this volume). In essence, the method works because, on the basis stellar evolution theory, we relate star counts in selected regions of the CMD to the mass of the stellar population which generated them. Since different regions of the CMD are populated by stars of different ages, the stellar counts speak for the mass that went into stars as a function of time. However, there are regions in the CMD which, sampling stars from a large age range, only yield integrated information. In this paper I will anticipate some results of an investigation of the potentials and the limitations of the stellar evolution theory for reconstructing the SFH. I will consider stellar populations with an age spread, but a fixed metallicity. I will also just focus on the number counts of stars in Post Main Sequence (PMS) evolutionary phases. Often these stars occupy the brightest portions of the observational CMDs. In addition, for this kind of stars a straightforward relation applies between the counts and the mass of the parent population.

### 2. The Number-Mass connection

For an Simple Stellar Population (SSP), i.e. a collection of single stars all with the same age ( $\tau$ ) and metallicity ( $Z$ ), the number of stars in the  $j$ -th PMS evolutionary phase is well approximated by (Renzini 1981):

$$\Delta N_j^{SSP} = \phi(M_{TO}) |\dot{M}_{TO}| \Delta t_j \quad (1)$$

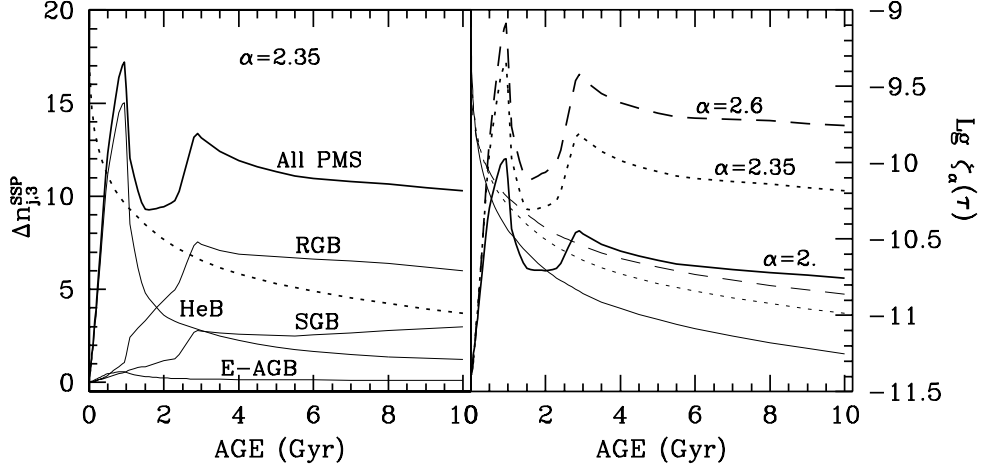


Figure 1. Left panel: the production of PMS stars of SSPs with  $M_{>0.6}^{SSP}=1000M_{\odot}$  for  $\alpha=2.35$ . The thick line refers to the total PMS; the thin lines to the individual phases: sub-giant branch (SGB), red giant branch (RGB), central Helium burning (HeB), double shell burning up to the first thermal pulse (Early AGB, E-AGB). The dotted line shows the specific evolutionary flux (right scale). Right panel: total PMS production (thick lines) and specific evolutionary flux (thin lines) for three values of  $\alpha$ . The linetype encoding is labelled.

where  $M_{TO}$  is the turn off mass,  $\dot{M}_{TO}$  is its time derivative,  $\Delta t_j$  is the lifetime of the PMS phase considered, and  $\phi(M_{TO})$  is the Initial Mass Function (IMF) by number evaluated at the turn-off mass.

I characterize the SSP for its total mass in the range  $0.6-120 M_{\odot}$  ( $M_{>0.6}^{SSP}$ ):

$$M_{>0.6}^{SSP} = \int_{0.6}^{120} \phi(M) dM = A \int_{0.6}^{120} M^{1-\alpha} dM = A / f_{\alpha} \quad (2)$$

having assumed a single slope power law for the IMF in the range  $0.6-120 M_{\odot}$ . In this notation, Salpeter IMF corresponds to  $\alpha=2.35$

The scaling of the number of PMS stars with the mass of the parent population then becomes:

$$\Delta N_j^{SSP} = M_{>0.6}^{SSP} \zeta_{\alpha} \Delta t_j = M_{>0.6}^{SSP} \times \Delta n_j^{SSP} \quad (3)$$

where  $\zeta_{\alpha} = f_{\alpha} M_{TO}^{-\alpha} |\dot{M}_{TO}|$  is the *specific evolutionary flux*, i.e. the number of stars leaving the MS per unit time per unit mass of the parent population. The quantity  $\Delta n_j^{SSP}$  is the *specific production of PMS stars* in the  $j$ -th evolutionary phase of the SSP with age  $\tau$  and metallicity  $Z$ , such that its turn off mass is  $M_{TO}$ . All factors in equation 3 depend on  $\tau$  and  $Z$ ; the dependence on the IMF is included in  $\zeta_{\alpha}$ .

The behaviour of the specific production of PMS stars as a function of the SSP age is shown in Fig. 1 for the set of tracks by Fagotto et al. (1994) with  $Z=0.004$ . The trend with age results from two competing effects: the temporal

decrease of the specific evolutionary flux as the population ages (dotted line in the left panel), and the increase of the duration of specific PMS stages.

For young SSPs (up to  $\approx 1$  Gyr) the specific production of PMS objects increases: the lengthening of the lifetimes prevails, and it's by far driven by the helium burning lifetime.

There is a sharp maximum in  $\Delta n_j^{SSP}$  at  $\approx 1$  Gyr: this is due to the fact that SSPs around this age have the longest helium burning lifetime (e.g. Sweigart, Greggio, & Renzini 1990; Girardi & Salaris 2001).

A second maximum appears at  $\approx 3$  Gyr, caused by the lengthening of the RGB lifetime. After this epoch the specific production of PMS stars mildly decreases with increasing age, as the RGB lifetime levels off.

The right panel of Fig. 1 illustrates the impact of the IMF slope on  $\Delta n_j^{SSP}$ . Older than a few hundred Myr, steeper slopes correspond to a larger number of PMS stars at fixed  $M_{>0.6}^{SSP}$ , reflecting the larger stellar evolutionary flux.

I now pass to consider the location in the CMD where these PMS stars are to be counted. Fig. 2 shows the magnitude range covered by PMS stars of SSPs with ages from 10 Myr to 10 Gyr. The Fagotto  $Z=0.004$  tracks in combination with the Bessel, Castelli and Pletz (1998) model atmospheres with  $[M/H] = -0.5$  have been used to produce this plot. Different shading refer to different PMS phases (see caption).

There is a well defined  $M_I - \tau$  relation for helium burners up to  $\approx 1$  Gyr, that is the age at which the Red Giant Branch develops to full extension (RGB phase transition). Thereafter the He burning is spent at virtually the same luminosity, independent on age.

In the intermediate age regime, the luminosity at the 1st AGB thermal pulse can be used to age-date the SSPs. This is at the basis of the AGB-tip age dating, although the location of the tip itself is uncertain due to our poor knowledge of the mass loss processes during the AGB evolution.

Beyond 1–2 Gyrs there's no bright feature that betrays the age of the SSP. To age-date the SSP we need to sample as deep as the RGB base. A notable exception is the presence of blue horizontal branch stars, but the corresponding age-dating is uncertain because the color distribution of these stars is sensitive to various poorly understood effects (see e.g. the second parameter problem (Renzini & Fusi Pecci 1988)).

### 3. Composite Stellar Populations

Having introduced the basic ingredients, I now pass to examine the connection between stellar counts in magnitude bins on the CMD of stellar populations with an age range, and their mass. For such Composite Stellar Population (CSP) eq. (3) becomes:

$$\Delta N_j^{CSP} = \int_{\tau_n}^{\tau_x} \dot{M}(\tau) \Delta n_j^{SSP} d\tau \quad (4)$$

where the subscript  $j$  now refers to the magnitude bin,  $\dot{M}(\tau)$  is the star formation rate (SFR) at the age  $\tau$ , and the integration is performed over the age range contributing to the counts in the  $j$ -th bin.

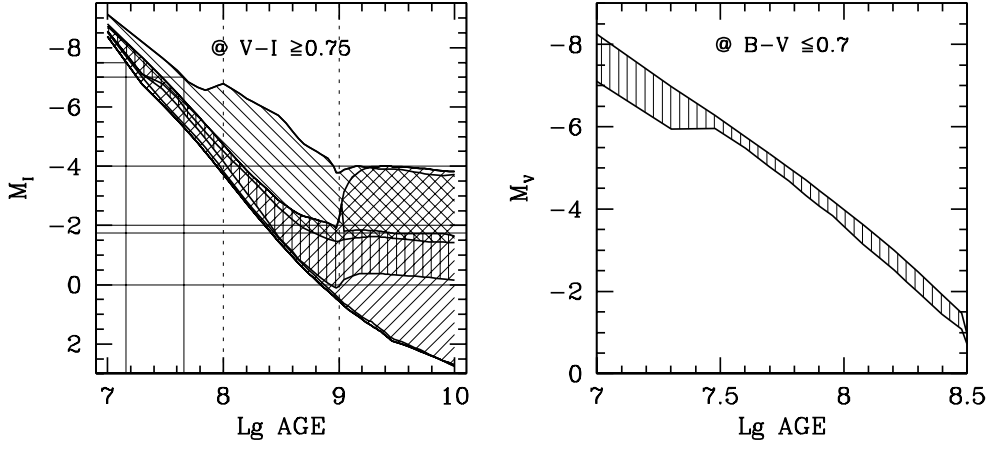


Figure 2. Magnitude range covered by red (left panel) and blue (right panel) PMS stars of SSPs with ages between 10 Myr and 10 Gyr. The color selection is labelled in each panel. Vertical shading refers to HeB; slanted shading to RGB (angle=+45°) and E-AGB (angle=-45°) stars.

The brightest regions of the CMD sample a relatively small range of ages. In this regime:

$$\Delta N_j \simeq \langle \dot{M} \rangle_{\tau_j} \Delta n \rangle_{\tau_j} \Delta \tau_j \quad (5)$$

where the SFR and the specific productions are evaluated at the typical age  $\tau_j$  sampled by the  $j$ -th magnitude bin, and  $\Delta \tau_j$  is the intercepted age range. As long as  $\Delta \tau_j$  is small (i.e. the position of the stars on the CMD varies steeply with their age) the luminosity function (LF) gives a detailed description of the star formation rate. Inspection of the left panel of Fig. 2 shows that this is the case only for the brightest portion of the red LF. Magnitude bins fainter than  $M_I \sim -6$  already collect E-AGB stars from a large age range. This problem is not present in the blue part of the CMD (right panel of Fig. 2), where  $\Delta \tau_j$  remains small up to a few hundred Myrs. Thus counts of blue helium burners give a fair indication of the SFR over this age range (Dohm-Palmer et al. 1997).

For older stellar populations, the bright portion of the CMD yields basically integrated information, as can be appreciated from Fig. 2. I turn then to consider the specific production of objects in a region of the CMD from a CSP:

$$\Delta n_j^{CSP} = \frac{\int_{\tau_n}^{\tau_x} \dot{M}(\tau) \Delta n_j^{SSP} d\tau}{\int_{\tau_n}^{\tau_x} \dot{M}(\tau) d\tau} = \langle \Delta n_j^{SSP} \rangle_{\dot{M}_\tau} \quad (6)$$

The specific production of  $j$ -type stars of a composite stellar population with a range of ages is the weighted mean of the specific productions of the SSPs, with the weights given by the SFR in the relevant age range. The star counts in a region of the CMD divided by  $\Delta n_j^{CSP}$  yields the mass that went into stars in the age range corresponding to the selected region of the CMD. It is thus important to see how this quantity varies under different assumptions for

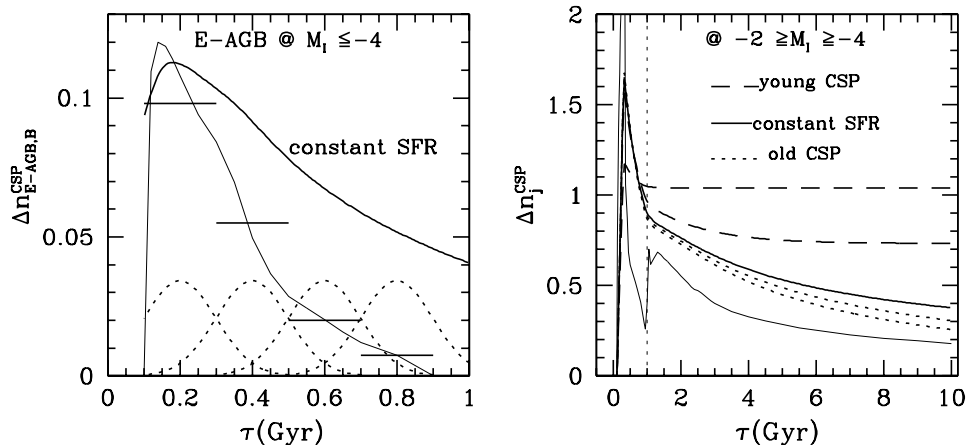


Figure 3. Production of stars from SSPs (thin lines) and CSPs (thick lines) with  $M_{>0.6}^{SSP}=1000M_{\odot}$  and  $\alpha=2.35$ . The left panel refers to E-AGB stars brighter than the RGB Tip, which are produced at ages between 0.1 and 0.9 Gyr in the adopted tracks. The right panel shows the production of stars with  $V-I \geq 0.75$  and  $-2 \geq M_I \geq -4$ . See text for more details.

the SFH. In the following I will consider the stellar counts in the red portion of the CMD.

The left panel of Fig. 3 illustrates the specific production of E-AGB stars brighter than the RGB tip (in the I band) for a variety of SF histories in the age range from 0.1 to 0.9 Gyr. The thick horizontal lines show the level of  $\Delta n_j^{CSP}$  for bursts of SF, modelled as gaussian distributions centered on progressively older ages, all with a 0.1 Gyr age dispersion (dotted lines). The thick continuous line, instead, shows  $\Delta n_j^{CSP}$  as a function of the maximum age of the CSP, for a family of SF episodes all occurred at a constant rate up to  $\tau_n = 0.1$  Gyr.

$\Delta n_j^{SSP}$  decreases rapidly with age: the older the stellar population, the more mass we have to put into stars to account for a given observed number of bright E-AGB stars.

The ratio between the mass of the CSP and the star counts depends on the age and the age limits of the SF episode considered. On the other hand the luminosity and colour of the AGB stars can be used to rank their age distribution, so that the uncertainty in the derived CSP mass can be estimated within a factor of a few.

The right panel of Fig. 3 shows the specific production of stars in the bin  $-2 \geq M_I \geq -4$ , which collects young helium burners, E-AGB intermediate age and old (AGB + RGB) bright stars (see Fig. 2). In this magnitude bin,  $\Delta n_j^{SSP}$  is very large for the young Helium burners, temporarily drops at intermediate ages (where the SSP only yield AGB stars), and has a second peak at the RGB phase transition. For ages older than  $\approx 1$  Gyr,  $\Delta n_j^{SSP}$  is only mildly varying over the whole range of ages considered. It follows that, in  $-2 \geq M_I \geq -4$ , the specific production of stars from CSP with  $\tau_n \geq 1$  Gyr only marginally depends on the age range.

The impact of the presence of young stars ( $\tau_n \leq 1\text{Gyr}$ ) in this magnitude bin is illustrated by the thick lines for a variety of SFHs. Specifically, the dashed lines correspond to an age distribution  $\propto e^{-\tau/\tau_0}$ ; the solid line to a constant SFR; the dotted line to an age distribution  $\propto e^{\tau/\tau_0}$ . The ratio of mass in stars younger than 1 Gyr to the mass in stars with ages between 1 and 10 Gyr is 5 (upper dashed), 1 (lower dashed), 0.1 (solid), 0.05 (upper dotted) and 0.02 (lower dotted). It can be seen that, if the CSP maximum age is older than the RGB phase transition (which gives well defined signature on the CMD, i.e. the RGB tip), the specific production is not very sensitive to the SF history and age limits. Again, the uncertainty of the conversion of stellar counts to total mass of the parent population can be estimated around a factor of a few. Similar considerations hold for a magnitude range which samples the helium burners (e.g.  $0 \geq M_I \geq -1.75$  in Fig. 2).

To summarize:

- The bright portion of the LF of PMS stars allows to recover the SFH with a fair degree of detail, up to ages of a few  $10^8$  years.
- For older ages, the specific production of stars in the various regions of the CMD depends on the age limits and on the SFR law of the CSP. It is however possible to estimate the total mass of the CSP within a factor of a few, for an assumed IMF slope.

On the average, for Salpeter IMF one gets approximately 1 E-AGB stars brighter than the RGB Tip every 20000  $M_\odot$ , 1 (red) star in  $-2 \geq M_I \geq -4$  every 2000  $M_\odot$  and 1 (red) star in  $0 \geq M_I \geq -1.75$  every 200  $M_\odot$  of the parent population (in stars more massive than  $0.6 M_\odot$ ).

The best way to decode the stars' distribution on the CMD in terms of SFH is by computing synthetic CMDs, which account for the stellar evolution, number statistics and observational uncertainties. In addition, the simulations allow to benefit of the information from the MS phase, and to cross check the star counts in different CMD regions which sample the same ages. Nevertheless, the Number-Mass relation illustrated here offers a quick-look tool to picture the SF history from an observational CMD, as well as theoretical support for the results we achieve through the construction of synthetic CMDs.

## References

- Bessel, M. S., Castelli, F., & Pletz, B. 1998, *A&A*, 337, 321  
 Dohm-Palmer, R. C., Skillman, E. D., Saha, A., Tolstoy, E., Mateo, M., Gallagher, J., Hoessel, J., Chiosi, C., & Doufour, R. J. 1997, *AJ*, 114, 2527  
 Fagotto, F., Bressan, A., Bertelli, G., & Chiosi, C. 1994, *A&AS*, 105, 29  
 Girardi, & Salaris, M. 2001, *MNRAS*, 323, 109  
 Renzini, A. 1981, *Ann. Phys. Fr.*, 6, 87  
 Renzini, A., & Fusi Pecci F. 1988, *ARA&A*, 26, 199  
 Sweigart, A. V., Greggio, L., & Renzini, A. 1990, *ApJ*, 364, 527